FINITE ELEMENT-BASED ASSESSMENT OF AXIAL COMPRESSION-INDUCED BUCKLING IN X60 STEEL PIPELINES

Mohammed Amine KHATER*[1], Chaaben ARROUSSI[2], Sid Ahmed MEMCHOUT[3]
[1] *Laboratoire de Recherche en Technologie de Fabrication Mécanique, École Nationale Polytechnique d'Oran M.A, Oran El M'Naouer, Algérie*
[2] *LPTPM, Departement of Mechanical Engineering, Faculty of Technology, Hassiba BenBouali University of Chlef, P.O. Box. 151 Hay Salem, 02000 Chlef, Algeria.*
[3]*Laboratoire de Physique des Couches Minces et Matériaux pour l'Electronique, Université d'Oran 1, Ahmed Ben Bella, BP 1524, El M'naouar 31100 Oran, Algeria.*
E-mail: m-amine.khater@enp-oran.dz*

AJME 2025, 23 (3); https://doi.org/10.5281/zenodo.17218061

***ABSTRACT**: This study examined the buckling resistance of an X60 steel pipe under axial compressive loading using finite element analysis. A 3-dimensional numerical model was created to explore the parametric influences on the buckling behavior of the pipeline. These parameters encompassed the pipeline geometry (including outer diameter and wall thickness), internal pressure, and mechanical properties of the steel (yielding strength). The obtained results show that the critical buckling load of the pipeline is primarily affected by the outer diameter and the thickness of the pipe, as well as by internal pressure and mechanical properties of the steel, such as the yield stress. The comparison of results with the analytical model reveals a good agreement between the mechanical and analytical results in the case of outer diameter and wall thickness, but there is a large error in the case of yield stress.*

***KEYWORDS**: X60 steel pipeline; Buckling; Critical buckling load; Finite element modeling.*

1 INTRODUCTION

The growth of population and industrial sectors in any nation leads to an increased demand for petroleum products [1]. When demand exceeds supply, addressing it requires either discovering new resource locations or exporting from surplus ones [2]. With the growing demand and the discovery of new crude oil and natural gas resources, the manufacturing industry has increasingly focused on their transportation [3]. Continuous transportation over long distances, often necessitated by these factors, is best achieved through pipelines [4]. Pipelines play an important role in securely and efficiently transporting a variety of energy products. Specifically, natural gas pipelines constructed from high-strength steels with large diameters and high operating pressures offer significant economic advantages [5]. Data indicates that increasing the strength level of pipeline steel from X60 to X80 grades can result in a construction cost savings of 7% [6]. Corrosion stands out as a primary mechanism capable of triggering pipeline failure. During the operation of oil and gas pipelines, impurities like sulfide, chloride, and water can be present in the transported fluid, leading to internal corrosion. Additionally, external corrosion may arise from the electrochemical interaction between pipeline steel and the surrounding soil environment [7]. Furthermore, heat exchange commonly transpires among the conveyed fluid, the pipeline, and the soil, potentially hastening the corrosion process of the pipelines [8]. For comparison, corrosion accounted for as much as 24% of pipeline accidents on pipelines regulated by the European Gas Pipeline Accident Data Organization from 2004 to 2013 [9]. Transmission pipelines occasionally traverse geotechnically unstable areas, Geohazards like earthquakes, faults, longitudinal landslides, and others can impose an axial compressive load on these pipelines, leading to local buckling at corrosion defects [10] .Extensive efforts have been undertaken to tackle this issue by establishing standards and devising models to compute the critical failure pressure of corroded pipelines [11].Utilizing finite element method (FEM) analysis and simplified corrosion defect geometries, pipeline damage prediction is widely acknowledged as the most precise approach for estimating failure pressure and the damage of pipelines, with different positions of defects and under different temperatures degree. This method is

commonly employed to assess the accuracy of established burst models [12-14]. Extensive research has been conducted on the buckling behavior of cylindrical thin-wall structures like pipelines subjected to axial compression loads [15]. Based on Donnell shallow shell theory and assuming a membrane pre-buckling state, a classical model has been developed to predict the elastic buckling load of these thin-wall cylinders [16].

This study aims to investigate the effect of different geometrical parameters on the critical buckling load of a pipe under axial compression. The buckling resistance of an X60 steel pipe was examined using advanced finite element analysis. Key parameters such as outer diameter, wall thickness, internal pressure, and mechanical properties like yield strength were analyzed. A comparison with analytical models was made to examine the accuracy of the numerical approach.

2 ANALYTICAL MODEL

Extensive research has been conducted on the buckling behavior of cylindrical thin-wall structures, particularly pipelines, subjected to axial compression load. A classical model for predicting the elastic buckling load of such cylinders was proposed based on the Donnell shallow shell theory and the assumption of a membrane pre-buckling state. This model has been widely utilized in the prediction of elastic buckling load for thin-wall cylinders [17]:

$$F_{cyl} = \frac{2\pi E t^2}{\sqrt{3(1-v^2)}}$$

In the context of thin-wall cylindrical structures, the elastic critical buckling load, denoted as F_{cyl}, can be determined using the Young's modulus E, Poisson's ratio (v), and the wall thickness (t) of the structure. However, for cylindrical structures with a thick wall thickness, their failure typically occurs within the elastic-plastic range, and the governing mode of failure is plastic collapse. To assess the critical axial compression, load that causes yielding of the structure, defined as the reference buckling load (F_{ref}), an empirical equation is commonly employed. This equation serves as a practical tool for calculating F_{ref}, thus facilitating the analysis of thick-walled cylindrical structures in the elastic-plastic regime [18]:

$$F_{ref} = \pi D t \sigma y$$

In the context of cylindrical structures, wherein D is denoted the outer diameter (e.g., pipe outer diameter), t represents the wall thickness of the pipe, and σy stands for the yield strength of the structural material, the aforementioned methods primarily serve to calculate the critical buckling load. These methods are specifically applied to pipelines that are devoid of corrosion and other types of defects and are subjected to axial compression.

3 MATERIAL PROPERTIES

In this research study, numerical analyses were conducted to examine the buckling behavior of the X60 pipe, as illustrated in Figure 1.

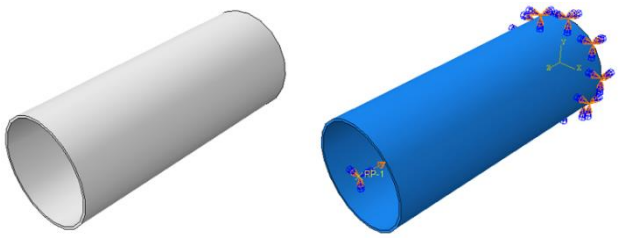

Fig. 1 Geometrical model of pipe

To accurately reproduce the buckling response, the true stress-strain curve obtained from a uniaxial tensile test was utilized. For the X60 pipeline steel, the corresponding yield stress and ultimate stress were determined to be 415Mpa and 590Mpa, respectively. The Young's modulus of the material was found to be 210000Mpa. The true stress-strain curve employed for numerical modeling is presented in Figure 2.

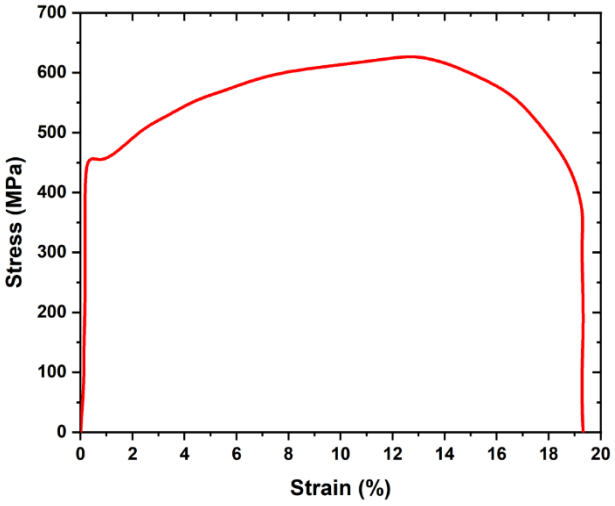

Fig. 2 Engineering stress- strain curve for X60 steel [19]

The numerical simulation was conducted utilizing the commercial software ABAQUS. In modeling the buckling behavior of pipes and circular hollow sections (CHS), in the present study, a 3D model of the pipe was generated, incorporating the geometric details represented by the outer diameter (D), wall-thickness (t), and axial

length (L). Figure 3 illustrates the resulting 3D model. The pipe model used in the analysis is depicted schematically. Boundary conditions were carefully imposed at each end of the pipe model to prevent any end collapse. One of the end collars was fixed in all degrees of freedom, preventing any rotations or translations. The reference point was established at the other end collar. This reference point (the loading end collar) was positioned at the free cross-section and subjected to a negative axial displacement along the longitudinal direction. This arrangement was implemented to induce axial compression load. The pipe segment was discretized using the C3D8R element. This choice was driven by its capability to accurately capture the geometry, deformations, and stress distributions while ensuring computational efficiency. Additionally, the NLGOM (Nonlinear Geometric Option Method) was enabled in ABAQUS for all numerical analyses conducted in this study.

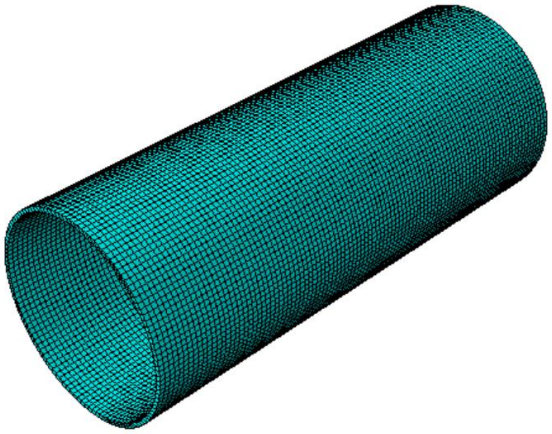

Fig. 3 Mesh view of studied model

accurately reproduce the buckling response, the true stress-strain curve obtained from a uniaxial tensile test was utilized. For the X60 pipeline steel, the corresponding yield stress and ultimate stress were determined to be 415Mpa and 590Mpa, respectively. The Young's modulus of the material was found to be 210000Mpa. The true stress-strain curve employed for numerical modeling is presented in Figure 2.

4 RESULTS AND DISCUSSION

4.1 Effect of type of mesh

The choice of mesh in computational elemental analyses significantly influences the distribution and quantity of nodes within the element, thereby affecting the overall mesh density in the structure. To attain convergence and optimize mesh density, a set of calculations was conducted using two mesh types: C3D8R (an 8-node quadratic brick element) and C3D10 (a 10-node quadratic tetrahedron element). Ensuring computational convergence involved stabilizing results, particularly the critical buckling load, aiding in the selection of the optimal number and type of elements, as illustrated in Figure 4.

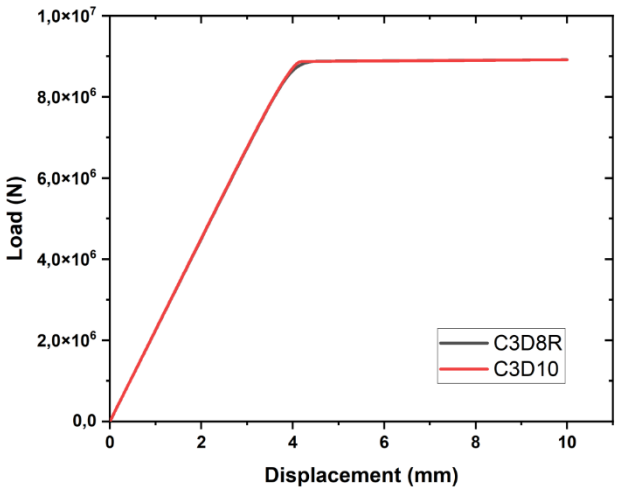

Fig. 4 Influence of mesh element type on the evolution of displacement –Load

4.2 Effect of thickness on buckling load

Figure 5 presents a comprehensive analysis of the critical buckling load (Fc) in pipes with varying wall thickness (t). The figure demonstrates a progressive increase in compressive load as the applied load intensifies. Upon reaching the maximum load, localized buckling occurs, causing the load to decrease while the displacement continues to increase until the pipe loses its loading capacity entirely. The value of the maximum load represents the critical buckling load, and the corresponding compressive load indicates the critical compressive displacement. Intriguingly, the investigation reveals that thicker pipes exhibit enhanced stiffness, leading to smaller displacements under a given load. This heightened stiffness results from the larger cross-sectional area and moment of inertia in thicker pipes, contributing to their remarkable resistance against deformation and consequent reduction in deflections. Conversely, thinner pipes display a different behavior as they tend to reach their yield point at lower loads, indicating a distinctive deviation from linearity. This characteristic can be attributed to the reduced capacity of thinner pipes to endure plastic deformation due to their lesser thickness. In

contrast, thicker pipes exhibit a higher load-carrying capacity, enabling them to withstand more

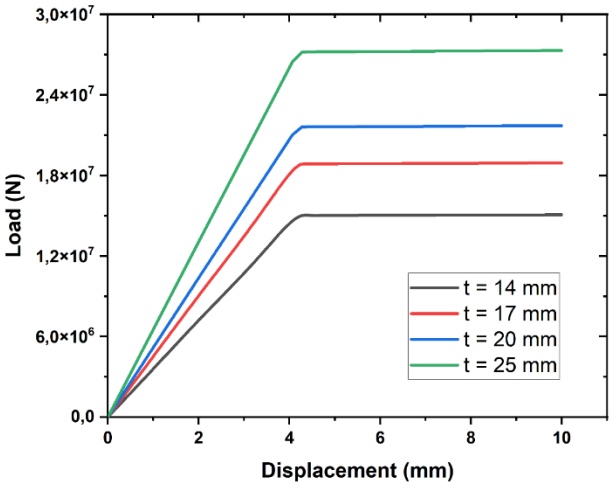

Fig. 5 Load versus Displacement for different thickness of pipe

substantial loads before encountering plastic deformation.

Figure 6 represents the prediction of critical buckling load in pipes with different thicknesses using two complementary approaches: finite element analyses and a theoretical equation. The primary objective is to evaluate the accuracy and agreement between the two methods and gain insights into the buckling behavior of pipes with varying thickness. Encouragingly, the comparison between the finite element results and theoretical predictions exhibited excellent agreement. The critical buckling load curves for pipes with different thicknesses closely overlapped, revealing a minimal gap between the two curves, effectively approaching zero. This remarkable alignment indicates that the theoretical equation accurately predicts the critical buckling behavior of pipes with varying thickness. The excellent agreement between the finite element analyses and theoretical predictions underscores the reliability of the theoretical equation in capturing the critical buckling behavior of pipes. The theoretical approach effectively accounted for the complex interactions between the pipe's geometry, material properties, and axial compression, resulting in consistent and accurate predictions across different thicknesses.

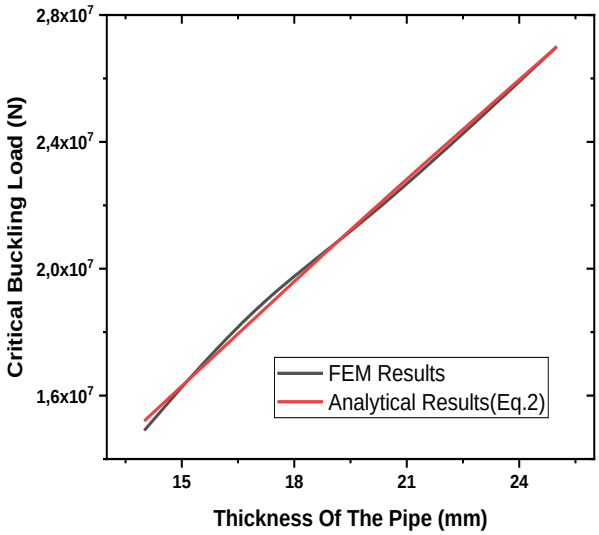

Fig. 6 Comparison between the analytical model and FEM results for different values of thickness.

4.3 Effect of diameter on buckling load

Figure 7 presents a comprehensive analysis of the critical buckling load (Fc) in pipes with varying outer diameter (D), while keeping a constant wall thickness (t) of 14 mm; the depicted figure illustrates a gradual rise in compressive load with increasing applied load. Upon reaching the maximum load, localized buckling ensues, leading to a subsequent decrease in load while the displacement continues to rise until the pipe ultimately loses its loading capacity. The value of this maximum load corresponds to the critical buckling load, and the corresponding compressive load signifies the critical compressive displacement. The results indicate that as the pipe's outer diameter increases, the critical buckling load also increases. This trend is primarily attributed to the improved stiffness of the pipe resulting from the larger outer diameter, consequently enhancing its resistance to compression. It is noteworthy, however, that the increased diameter simultaneously leads to higher hoop stress and von Mises equivalent stress within the pipe structure. These elevated stresses, in turn, reduce the pipe's capacity to resist buckling. Despite this, it is observed that the positive effect of increased diameter on stiffness and compression resistance plays a dominant role in influencing the buckling response of the pipe.

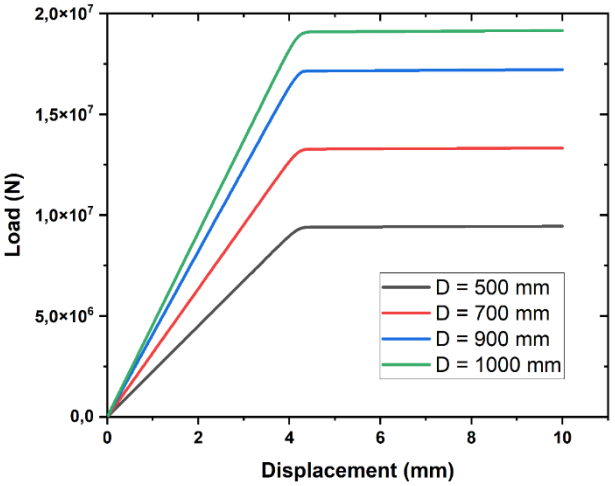

Fig. 7 Load versus displacement for different outer diameter of pipe.

Figure 8 represents a comprehensive comparison between the critical buckling loads of pipes under axial compression, as determined by two different methods: finite element analyses and a theoretical equation. The main objective was to evaluate the level of agreement between the two approaches and gain insights into the buckling behavior of pipes with different outer diameters. The comparison between the finite element analyses and theoretical predictions revealed an exceptional agreement. The critical buckling load curves for pipes with different outer diameters exhibited a minimal gap between them, indicating a remarkably close alignment between the two methods. The discrepancies were consistently negligible across the range of pipe outer diameters tested. The close agreement between the finite element analyses and theoretical predictions underscores the reliability of the theoretical equation in capturing the critical buckling behavior of pipes. The theoretical approach effectively accounted for the complex interactions between the pipe's geometry, material properties, and axial compression, resulting in highly accurate and consistent predictions.

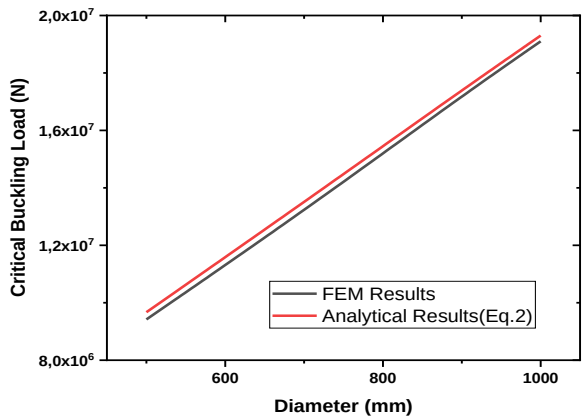

Fig. 8 Comparison between the analytical model and the FEM results for different outer diameter of pipe.

4.4 Effect of yield stress on buckling load

The buckling behavior of pipeline exhibits significant material nonlinearity, necessitating the consideration of X60 steel properties in the buckling analysis. This study incorporates the yield strength of X60 steel into the modeling process. Specifically, the effect of the yield strength is investigated by examining four groups of varying yield strengths, while the tensile strength remains fixed at 590Mpa. Other input parameters include a pipe outer diameter (D) of 500mm; pipe wall thickness (t) of 14 mm. Figure 9 reveals a nonlinear relationship between the critical buckling load (Fc) and the yield strength (σy). As the yield strength increases, Fc also rises, indicating an enhanced buckling resistance of the corroded pipeline.

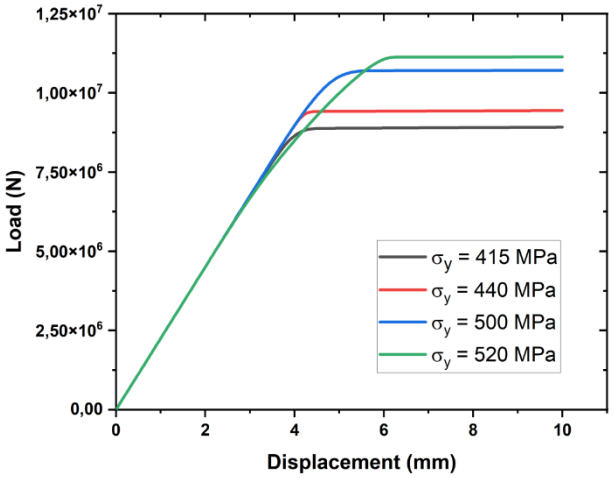

Fig. 9 Load versus displacement for different outer diameter of pipe.

In this research, we investigated the prediction of yield stress in pipes using two different approaches: finite element analyses and a theoretical equation. The main objective was to evaluate the accuracy of the theoretical equation compared to the more computationally intensive finite element analyses and understand the behavior of pipes under various loading conditions. Surprisingly, a substantial gap was observed between the yield stress curves obtained from finite element analyses and the theoretical equation. The theoretical predictions consistently underestimated the yield stress, leading to significant discrepancies between the two methods across different pipe configurations and loading conditions. The substantial gap between the finite element analyses and theoretical equation raises concerns about the accuracy of the latter in predicting the yield stress of pipes. The theoretical approach might not fully capture the complex stress distributions and

localized effects that occur in real-world scenarios, which are better captured through finite element analyses. Several factors could contribute to the observed discrepancies. The theoretical equation might neglect certain material behaviors, boundary conditions, or geometric complexities that significantly influence the yield stress in real pipes. Additionally, strain-hardening and strain-softening effects, which are common in materials undergoing plastic deformation, may not be accurately captured by the theoretical model.

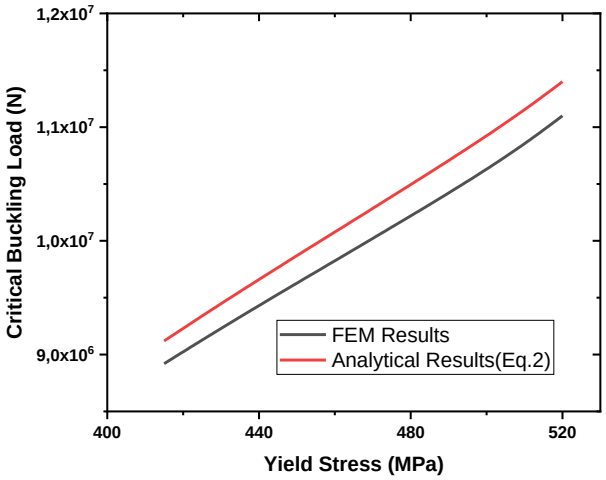

Fig. 10 Comparison between the analytical model and the FEM results for different values of yield stress of steel X60.

4.5 Effect of pressure on buckling load

The load-displacement curves for the pipe model with a nominal strain of n = 0.15 and D/t = 90 are depicted in Figure 11. It is evident from the curves that all specimens display a distinct maximum force. Notably, the maximum force decreases proportionally with the increment in internal pressure. Additionally, as the internal pressure rises, the pipe's cross-sectional area experiences additional stress due to the internal pressure acting on the pipe wall. This stress counteracts the applied axial load, leading to a reduction in the maximum force exhibited by the pipe. The increased internal pressure results in increased hoop stress on the pipe wall, causing it to withstand less axial load before yielding or buckling occurs, also the rising of internal pressure lead to the pipe becomes more susceptible to plastic deformation, which leads to increased displacements at the point of maximum force. As the pipe undergoes plastic deformation, it experiences a higher degree of yielding and permanent deformation, contributing to greater displacements at the critical load.

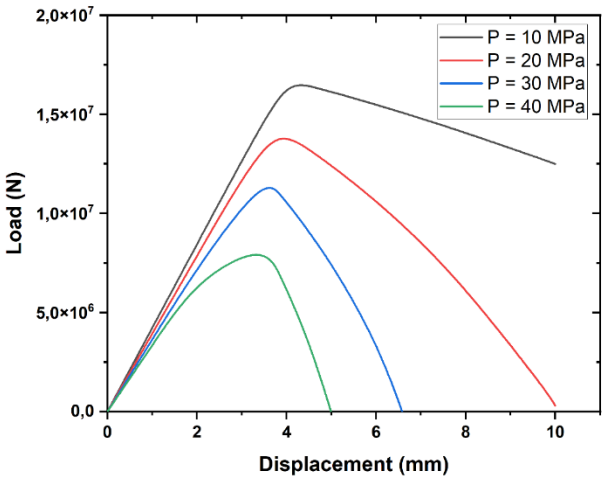

Fig. 11 Load versus displacement for different values of internal pressures.

The figure depicted the linear fit of the critical buckling load in terms of internal pressure. As the internal pressure increases, the critical buckling load decreases in a linear manner. This finding indicates that the buckling behavior of the structure is influenced primarily by internal pressure, and the two variables exhibit a consistent linear correlation. Using a fitting technique, we derived a formula to describe the buckling behavior, representing the net critical load as a function of pressure variation. The resulting formula is illustrated in Figure (12) as follows:

$$F(p) = -271100\,P + 1.9485 \times 10^{7}$$

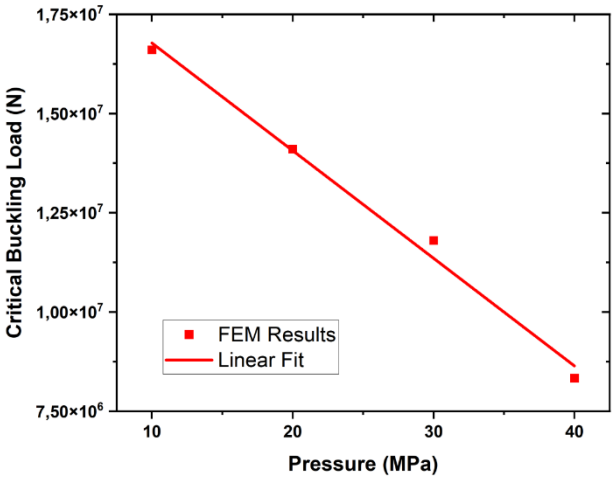

Fig. 12 Relationship between the internal pressures and the critical buckling load.

5 CONCLUSION

The buckling phenomena discovered in the study gives important information on the structural behavior of X60 steel pipes under axial compressive force. Finite element analysis and parametric exploration have been used to study numerous parameters impacting buckling behavior, such as

pipeline shape, internal pressure, and steel mechanical characteristics.

The findings show the crucial role of outer diameter and wall thickness in influencing the pipeline's buckling resistance. Additionally, internal pressure and mechanical qualities, notably yielding strength, have a major impact on the critical buckling load.

A comparison with analytical models showed good agreement in terms of outer diameter and wall thickness, but differences in predicting buckling behavior due to yield stress. In addition, the shape of the tube undergoes significant changes in response to variations in internal pressure.

6 REFERENCES

[1] Chang, X. P., Fan, J. M., Qu, C. J., & Li, Y. H. (2023). Coupling vibration of composite pipe-in-pipe structure subjected to gas-liquid mixed transport by means of green's functions. *Mechanics of Advanced Materials and Structures*, *30*(8), 1604–1623.
https://doi.org/10.1080/15376494.2022.2037794

[2] Cheng, F., 2016. Monitor safety of aged fuel pipelines.Nature529,156–156.
https://doi.org/10.1038/529156e

[3] Wang, Y., Zhang, P., Qin, G., 2019. Non-probabilistic time-dependent reliability analysis for suspended pipeline with corrosion defects based on interval model. Process Safety and Environmental Protection,124,290–298.
https://doi.org/10.1016/j.psep.2019.02.028

[4] Ríos-Mercado, R.Z., Borraz-Sánchez, C., 2015. Optimization problems in natural gas transportation systems: A state-of-the-art review. Applied Energy 147,536–555.
https://doi.org/10.1016/j.apenergy.2015.03.017

[5] Zhang, K., Bokka, H.K., Lau, H.C., 2022. Decarbonizing the energy and industry sectors in Thailand by carbon capture and storage. Journal of Petroleum Science and Engineering 209, 109979. https://doi.org/10.1016/j.petrol.2021.109979

[6] Qian, G., Niffenegger, M., Zhou, W., Li, S., 2013. Effect of correlated input parameters on the failure probability of pipelines with corrosion defects by using FITNET FFS procedure. International Journal of Pressure Vessels and Piping 105–106,19–27.
https://doi.org/10.1016/j.ijpvp.2013.02.004

[7] Zvirko, O., Mytsyk, B., Nykyforchyn, H., Tsyrulnyk, O., & Kost', Y. (2023). Application of the various methods for assessment of in-service degradation of pipeline steel. *Mechanics of Advanced Materials and Structures*, *30*(24), 5058–5067.
https://doi.org/10.1080/15376494.2022.2111732

[8] Zhao, Z., Zhou, S., Yang, Y., Zhao, B., Gao, T., & Yu, D. (2023). Predictions of loading capacity and stiffness of corroded circular steel tubes based on artificial neural networks. *Mechanics of Advanced Materials and Structures*, *30*(19), 4040–4051.
https://doi.org/10.1080/15376494.2022.2087243

[9] Qian, G., Cao, Y., Niffenegger, M., Chao, Y.J., Wu, W., 2018. Comparison of constraint analyses with global and local approaches under uniaxial and biaxial loadings. European Journal of Mechanics - A/Solids 69, 135–146.

[10] Keshtegar, B., el Amine Ben Seghier, M., 2018. Modified response surface method basis harmony search to predict the burst pressure of corroded pipelines. Engineering Failure Analysis 89,177–199.
https://doi.org/10.1016/j.engfailanal.2018.02.016

[11] Mokhtari, M., Melchers, R.E., 2018. A new approach to assess the remaining strength of corroded steel pipes. Engineering Failure Analysis 93,144–156.
https://doi.org/10.1016/j.engfailanal.2018.07.011

[12] Arroussi, C., Belalia, A., & Hadj Meliani, M. (2024). Numerical analyses on limit load of X60 pipe elbow in different internal corrosion-damaged positions under combined internal pressure and in-plan bending moment. International Journal on Interactive Design and Manufacturing (IJIDeM), 1-11. https://doi.org/10.1007/s12008-024-01736-y

[13] Arroussi, C., Belalia, A., & Meliani, M. H. (2024). Temperature effects on the resistance capacity of API X60 pipe elbow under bending moment using X-FEM method. Journal of Mechanical Science and Technology, 1-9. https://doi.org/10.1007/s12206-024-0114-0

[14] Arroussi, C., Belalia, A., & Meliani, M. H. (2023). Effects of composite and metallic patch on the limit load of pressurized steel pipes elbow with internal defects under opening bending moment. Structural Monitoring and Maintenance, 10(3), 221. DOI: https://doi.org/10.12989/smm.2023.10.3.221

[15] Forero, A.B., Ponciano, J. a. C., Bott, I.S., 2014. Susceptibility of pipeline girth welds to hydrogen embrittlement and sulphide stress cracking. Materials and Corrosion 65, 531–541. https://doi.org/10.1002/maco.201206574

[16] Ifayefunmi, O., 2016. Buckling behavior of axially compressed cylindrical shells: Comparison of theoretical and experimental data. Thin-Walled Structures98,558–564.
https://doi.org/10.1016/j.tws.2015.10.027

[17] Wang, H.K., Yang, Y., Xu, J.X., Han, M.X., 2019a. Effect of pitting defects on the buckling strength of thick-wall cylinder under axial compression. Construct. Build. Mater. 224, 226–241.

[18] Wang, Y.H., Zhang, P., Qin, G.J., 2019b. Non-probabilistic time-dependent reliability analysis for suspended pipeline with corrosion defects based on interval model. Process Saf. Environ. Protect. 124, 290–298.

[19] Araújo, B. A., Travassos, G. D., Silva, A. A., Vilar, E. O., Carrasco, J. P., & de Araújo, C. J. (2011). Experimental characterization of hydrogen embrittlement in API 5L X60 and API 5L X80 steels. Key Engineering Materials, 478, 34-39. https://doi.org/10.4028/www.scientific.net/KEM.478.34.

7 NOTATION

The following symbols are used in this paper:
F_{cyl} = the elastic critical buckling load;
F_{ref} = the reference buckling load;
t = the pipe wall thickness;
v = Poisson's ratio;
E = Young's modulus;
D = the pipe outer diameter;
F_c = the critical buckling load;
σy = the yield strength;
F_{ref} = the reference buckling load;
FEM=finite element method.